PERIÓDICO TCHÊ QUÍMICA
ARTIGO ORIGINAL

ESTUDO DE PROCESSOS DE DEFORMAÇÃO DE MATERIAIS PLÁSTICOS USANDO PROCESSAMENTO DE IMAGEM DIGITAL

INVESTIGATION OF PROCESSES OF DEFORMATION OF PLASTIC MATERIALS WITH THE HELP OF DIGITAL IMAGE PROCESSING

ИССЛЕДОВАНИЕ ПРОЦЕССОВ ДЕФОРМАЦИИ ПЛАСТИЧНЫХ МАТЕРИАЛОВ С ПРИМЕНЕНИЕМ ЦИФРОВОЙ ОБРАБОТКИ ИЗОБРАЖЕНИЙ

BODRYSHEV, Valeriy V.[1*]; BABAYTSEV, Arseniy V.[2]; RABINSKIY, Lev N.[3];

[1] Moscow Aviation Institute (National Research University), Department of Engineering Graphics, Moscow – Russian Federation

[2] Moscow Aviation Institute (National Research University), Institute of General Engineering Training, Research Department No. 9, Moscow – Russian Federation

[3] Moscow Aviation Institute (National Research University), Institute of General Engineering Training, Moscow – Russian Federation

** Correspondence author*
e-mail: NioBVV@mail.ru

Received 20 October 2019; received in revised form 14 November 2019; accepted 14 November 2019

RESUMO

Atualmente, uma ampla gama de trabalhos está em andamento para criar métodos de correlação usando algoritmos apropriados. Isso é especialmente útil na construção de vetores de deslocamento para avaliar a deformação de materiais com o estabelecimento de correspondência entre as seções de duas imagens, calculando as funções de correlação cruzada e procurando um extremo. O objetivo deste trabalho foi desenvolver um método para avaliar o mecanismo de destruição do material de acordo com a análise da imagem fotográfica pelo parâmetro de intensidade da imagem utilizando a análise multivariada da relação entre a intensidade da imagem. Além disso, este método deve ser usado com a ajuda de análises multivariadas (análise de múltiplos fatores) das relações entre intensidade da imagem e rugosidade da superfície, revelando a geometria da área (volume) de deformação sob várias condições operacionais. O método digital de processamento de fotografias (quadros de vídeo) foi utilizado para estudar a microestrutura e a superfície dos materiais pelo critério de intensidade da imagem durante os testes de deformação mecânica. Os parâmetros quantitativos da intensidade da imagem são comparados com a estrutura do material, a rugosidade da superfície antes e após a destruição das amostras. As imagens utilizadas foram obtidas durante o teste mecânico de amostras de alumínio. Para garantir a confiabilidade dos resultados dos testes, foram testadas seis amostras do mesmo tipo. Um diagrama de tensão-deformação foi criado para cada amostra. Os diagramas de tensão-deformação dos testes mecânicos foram comparados com os diagramas de fotoanálise usando o método descrito acima. Os resultados correlacionaramm-se bem um com o outro, mas, diferentemente do experimento, onde a tensão é medida apenas no local do medidor de tensão, a fotoanálise fornece uma imagem completa da distribuição da tensão em toda a área da amostra. Além disso, foi realizada uma análise multivariada para avaliar as dimensões e formas geométricas dos elementos estruturais.

Palavras-chave: *fotografia (quadro de vídeo), estrutura do material, escala de cinzentos, rugosidade, teste de tração.*

ABSTRACT

As of now, many investigations are performed in order to develop methods of correlation with the help of relevant algorithms. This is especially helpfull for plotting vectors of displacements in order to estimate deformation of various materials, as well as to determine correspondence between sections of two images through calculation of the cross-correlating functions and to ensure seeking of the extremum. The aim of this study was to develop relevant method to estimate mechanism of fracture of materials in accordance with the data of analysis of a photographic image in respect of the parameter of the image intensity. In addition, this method is to be used with the help of the multivariate analysis (multi-factor analysis) of the interrelationship

DOI: 10.52571/PTQ.v16.n33.2019.880_Periodico33_pgs_865_876.pdf

between image intensity, surface roughness, and possibility to determination the geometrical parameters of the deformation area/deformation volume under different conditions of operation. Digital method of processing of photographs/video frames has been used in order to investigate microstructure and surface of materials in respect of criterion of the image intensity in the course of mechanical tests in accordance with deformations. Quantitative parameters of the image intensity were compared to the structure of material, as well as to the surface roughness before and after destruction of samples. The images used were obtained during mechanical testing of aluminium samples. To ensure the validity of the test results, six specimens of the same type were tested. A stress-strain diagram was drawn up for each specimen. Stress-strain diagrams from the mechanical tests were compared with those from the photo analysis using the method described above. The results correlate well with each other, but unlike the experiment, where the strain is measured only at the strain gauge location, the photo analysis provides a complete picture of the strain distribution over the entire specimen area. In addition, a multivariate analysis has been carried out to evaluate the geometric dimensions and shapes of the structure elements.

Keywords: *photograph (video frame), structure of material, grey colour gradation, roughness, tensile strength test.*

АННОТАЦИЯ

В настоящее время проводится большой спектр работ по созданию методов корреляции с применением соответствующих алгоритмов. Это особенно полезно для построения векторов перемещений для оценки деформации материалов, с установлением соответствия между участками двух изображений путем вычисления взаимно-корреляционных функций и поисков экстремума. Целью данной работы является разработка метода оценки механизма разрушения материала по данным анализа фотоизображения по параметру интенсивности изображения с привлечением многофакторного анализа связи между интенсивностью изображения. Кроме того, этот метод должен использоваться с помощью многомерного анализа (многофакторного анализа) взаимосвязей между интенсивностью изображения, шероховатостью поверхности, выявлением геометрии площади (объема) деформации при различных условиях эксплуатации. Цифровой метод обработки фотографий (видеокадров) был использован для исследования микроструктуры и поверхности материалов по критерию интенсивности изображения в процессе механических испытаний по деформациям. Сопоставлены количественные параметры интенсивности изображения со структурой материала, шероховатостью поверхности до и после разрушения образцов. Используемые изображения были получены во время механических испытаний образцов алюминия. Для обеспечения достоверности результатов испытаний были испытаны шесть образцов одного типа. Диаграмма напряжение-деформация была составлена для каждого образца. Диаграммы напряжения-деформации механических испытаний сравнивали с диаграммами фотоанализа с использованием метода, описанного выше. Результаты хорошо коррелируют друг с другом, но в отличие от эксперимента, где деформация измеряется только в месте расположения тензометрического датчика, фотоанализ дает полную картину распределения деформации по всей площади образца. Кроме того, был проведен многомерный анализ для оценки геометрических размеров и форм элементов конструкции.

Ключевые слова: *фотография (видеокадр), структура материала, градация серого цвета, шероховатость, испытание на растяжение.*

1. INTRODUCTION

Due to development of the high-quality recording photographic equipment and video equipment, as well as development of digital methods of the videodata processing in various branches of technology (Znamenskaya *et al.*, 2001; Bessonov *et al.*, 2013, Filippov and Proskokov, 2014; Belov *et al.*, 2014; Berezovskii *et al.*, 2015; Kobets *et al.*, 2016; Bodryshev and Morgunova, 2017a; Babaytsev *et al.*, 2017a; Formalev and Kolesnik, 2017; Formalev and Kolesnik, 2018; Bulychev *et al.*, 2018), there exists the possibility for development of the quick-operating and non-contact methods in order to estimate deformations of materials in various conditions of operation in respect of the parameter of the image intensity of photographs/video frames (Borynyak and Nepochatov, 2007; Volkov, 2010; Sodushkin *et al.*, 2011; Bodryshev and Morgunova, 2017b; Bodryshev, 2017; Bieda *et al.*, 2018; Babaytsev *et al.*, 2019; Ho *et al.*, 2019). This problem is the task of vital importance in the course of investigations of deformation processes and processes of destruction of the structurally nonuniform materials (metals, ceramic materials, composite materials and so on) (Rief *et al.*, 2017; Bodryshev and Morgunova, 2017a; Bulychev *et al.*, 2018; Dzioba and Lipiec, 2018; Rabinskiy *et*

al., 2019; Faraji and Torabzadeh, 2019; Hosdez *et al.*, 2019).

At the present time, many investigations are performed in order to develop methods of correlation with the help of relevant algorithms for plotting vectors of displacements in order to estimate deformation of various materials (Sodushkin *et al.*, 2011; Borodulin, 2013; Filippov and Proskokov, 2014; Bodryshev and Morgunova, 2017a; Bodryshev, 2017; Kang and Muhammad, 2017; Wu *et al.*, 2018; Babaytsev *et al.*, 2019), as well as to determine correspondence between sections of two images through calculation of the cross-correlating functions and to ensure seeking of the extremum (Görtan, 2017; Pushkarev et al., 2017; Iwamoto and Kanie, 2017; Yang *et al.*, 2018; Khotinov *et al.*, 2019; Muniandy, 2019; Wang *et al.*, 2019). Calculated values of the deformation parameters will be final results of such method. Investigations of various processes of destruction of plastic materials are described in this article. The article presents investigation of the problem of interrelationship between deformation of surfaces of various materials and the law of variation of the intensity of images of these surfaces.

Goal of the present article was to develop relevant method in order to estimate mechanism of fracture of materials in accordance with the data of analysis of a photographic image in respect of the parameter of the image intensity.

2. MATERIALS AND METHODS

Mechanical tensile strength tests have been performed in order to verify the proposed methodology. These tests were performed with the help of the Instron 5969 (produced of the Great Britain) equipment as well as with the help of the Bluehill 3 software. The sample has been captured and held with the help of special mechanical captures. Speed of performance of these tests has been established at the level of 1 mm/minute. All tests have been performed at room temperature. These tests have been performed with the help of 4 samples up to the moment of destruction of these samples. The samples were made as the platelets with following dimensions: 120 mm in length, 10 mm in width, and 1.4 mm in thickness. All samples were photographed before and after tests. The load – displacement diagram was constructed in accordance with results of these tests.

Photographs or video frames of the material structure of all samples are stored in the files, which have BMP or JPEG extensions. Quality of images is determined in accordance with quantity of pixels within the preassigned section in the range from 72 up to 400 pixels/inch (from 28.35 up to 157.48 pixels/cm).

Before and after tests, the entire area of relevant photograph of the sample under investigation is then splitted into discrete cells, which contain from 1 up to *k* pixels in horisontal direction (axis of abscissas *x*) and from 1 up to *m* pixels in vertical direction (axis of ordinates *y*). Dimension of the cell depends on the required precision of estimation in the course of investigation of the relevant photograph and this dimension must be the same in both variants. Function L=f(x,y) of intensities of images within a cell is quantitative characteristic of these intensities (that is, white colour level within a photograph). This function (in the case of a digital still photograph) is presented as the matrix of integers, which are reduced to the range of gradations from 0 up to 255 (quantisation) (Bodryshev and Morgunova, 2017a; Formalev and Kolesnik, 2017; Shtefan *et al.*, 2019). In the course of investigation of the obtained matrix it is very important to transform this matrix with the help of the coefficient of discreditation (Equation 1). In this case, $\Delta_{measured}$ and Δ_{actual} is share of dimension of components within a digital still photograph and actual value of this dimension, respectively.

Therefore, an image is presented as the two-dimensional function L(xy) along with construction of the relevant diagram, where *x* and *y* are coordinates of the cells within a photograph, while L is intensity of image (brightness) within the preassigned cells (Figure 1). The obtained data are presented in a graphical form as the three-dimensional model xyL (Figure 1b). Further processing of this model makes it possible to determine the following: laws of change of the L=f(x,y) in the longitudinal or transversal cross-sections; any coordinate in any point of the relevant diagram; distance between cells and so on. In the course of investigation of influence of length of the section ($H_{calculated}$), within which measurement of deformation is performed (Figure 2), it is very important to determine exact position of the point of deformation within the sample. Relative deformation ε is determined in accordance with the following expression (Equation 2). Where $H_{calculated\ 0}$ and $H_{calculated}$ is length of the deformation fixation within the initial sample and after destruction of this sample, respectively. It is worthy of note that destruction of material in the second variant (Figure 2b) was observed near the upper jaw for fixation of the

sample in the testing machine ($H_{apper\ part}$). In this case, section $H_{calculated}$ is situated in the lower part of the sample and relative deformation is only determined in accordance with the data in respect of tensile of the lower section of the relevant sample.

Figure 3 presents fracture diagram N-ε of the sample 1.1 (Figure 2). In this case, N is load upon the sample. A substantial zone of the material yielding is clearly visible. The following Figure 4 presents digital image of the sample 1.1 after destruction. Zone of the surface deformation near the point of destruction is clearly visible. It is important to determine the structure of this deformation. As concerns transversal direction, this deformation has the wave structure, which is characterised by the amplitude of variation of the image intensity value Equation 3, as well as by parameters of deformation of the relevant material (roughness). In this case $L_{max.Mi}$, $L_{min.Mi}$ are maximum and minimum values of intensity (respectively) within the i-th wave (which is under consideration) of the M-th cross-section.

There are good reasons to analyse the data on the amplitude of variation of the surface deformation of various materials Equation 4 as the criterion of the material deformation. In this case, h_{MaxMi}, h_{MinMi} respectively, are maximum and minimum values of the deformation height within the i-th wave (which is under consideration) of the M-th cross-section.

There are good reasons to perform comparison of these criterions in accordance with the data of the root-mean-square deviation SL and Sh of parameters L and h. For the M-th cross-section, we will have (Equations 5; 6). In this case, L_{Mk} and h_{Mn} is value of L within the k-th cell and value of h in the course of the i-th measurement of the M-th cross-section, respectively, while $\overline{L_M}$ and $\overline{h_M}$ are average values of these parameters. In addition, there are good reasons to analyse standard criterion R_z of the surface roughness as the criterion of deformation (Bodryshev, 2017; Bodryshev and Morgunova, 2017b; Babaytsev *et al.*, 2019).

It is recommended to use method of the contour analysis in order to determine geometrical parameters of sections of deformation near the zone of destruction (Borynyak and Nepochatov, 2007; Bodryshev, 2017). Section is characterised by availability of cells with the range of dispersion of the image intensity Equation 7. In this case, $L_{max.}$ and $L_{min.}$ are minimum and maximum values of the image intensity within the cells of digital display of the sample surface, respectively. The entire area of the section with the preassigned values of ΔL_1 is determined in accordance with the help of the receptor models, which ensure discretisation of space. The receptor method is based on the approximate representation of a geometrical object within the field/space of receptors. From the mathematical point of view, the receptor geometrical model is described by the multitude $A=\{a_{ij}\}$, where (Equation 8). It is assumed that receptor is in the unexcited state, if boundary of the section does not crosses this receptor, as well as if this receptor does not belong to the internal branch.

The obtained matrix, which contains the data "*1*", makes it possible to estimate boundaries of this section, as well as to determine its area. The entire area of the preassigned section S_i is determined with the help of summation of all n cells with parameter "*1*". Then this sum is to be multiplied by the area of one cell. This area is to be determined as the product of the cell width s_{cell} and height h_{cell} (Equation 9). Contour of the section is determined with the help of Freeman chain code (Borynyak and Nepochatov, 2007; Vinogradov, 2015; Bodryshev, 2017; Babaytsev *et al.*, 2017b; Kornev *et al.*, 2018; Rabinskiy and Tushavina, 2019; Rabinsky and Tushavina, 2019). It is reasonable to generalise results of the statistical analysis, which is to be performed with the help of the required quantity of samples on the condition of the preassigned kind of loading, in accordance with the statistical criterions.

3. RESULTS AND DISCUSSION:

On the basis of the data, which are contained in the matrices of digital display of samples and which are presented in Figure 2, Table 1 and Figure 5 present results of calculation of change of the relative deformation ε in the course of variation of the $H_{calculated}$ at different distances from the fixation jaws. It is obvious that relative deformation increases in the course of decrease of the distance $H_{calculated}$. In this case, we observe various kinds of dynamics of change in values of ε depending on position of the point of fracture. Therefore, issue of dependence of the ε value from the position of $H_{calculated}$ is the problem of vital importance.

Let us analyse dynamics of change in S_L and S_h values, as well as dynamics of change in the criterion of roughness R_z of sample 1.1. Figure 6 presents fixed cross-sections in the longitudinal and transversal directions for the

upper and lower parts of the sample, which was fractured in the conditions of tensile. Figure 7 presents diagram of change of the image intensity L in the longitudinal cross-section in the centre of the destroyed upper part of the sample (cross-section 6 of the upper part). Roughness of this cross-section was determined with the help of the Mitutoyo Surftest SJ-210 equipment. Chart of change of the roughness is presented in Figure 8 (diagram of the roughness measurement was constructed beginning from the upper end of the deformation section at the distance of 30 mm from the point of destruction). Construction of such charts makes it possible to determine the law of interrelationship between the parameters under investigation.

Comparisons in respect of SL values, as well as in respect of dispersion of roughness Sh have been performed in accordance with the following procedures (Figure 6):

1. Analysis of the data SL and Sh in the longitudinal cross-sections (1.5, 6, 9) of the upper and lower parts of the sample (of the samples).

2. Analysis of the data SL and Sh in the transversal cross-sections of the upper and lower parts of the sample (of the samples).

3. Group analysis of the data SL and Sh in the transversal and longitudinal cross-sections of the upper and lower parts of the sample (of the samples).

4. Performance of analysis of the data SL along with parameters of roughness Rz.

Relevant chart (Figure 9) presents dynamics of change of the data SL, Sh, Rz in the upper part of the fractured sample in the transversal cross-sections 2.5, 5.5, 6.5, 10, 20, and 30 mm (as an example). Clear trend of the interconnected correlation between these parameters is observed. It is possible to determine two sections in the range from 2.5 up to 5.5 mm, where change of SL, Sh, and Rz values is practically inessential, as well as the second section (more than 20 mm), where effect of deformation is an insignificant factor.

Results of performed investigations clearly demonstrate that deformation of surface within the zone of destruction is only determined by the effect of destruction as such, as well as that deformation depends on of the surface roughness of the initial sample to a lesser degree. As concerns the lower part of the sample (Figure 6b), dynamics of change of parameters is different as compared to the dynamics of the upper part (Figure 10) in a certain degree. It is possible that these data can be explained with the help of different "conditions" of deformation of these samples. As concerns the range from 5 up to 18 mm, values of Rz and Sh decrease in the form of waves and have inessential slope, while SL value has a substantial slope. It is reasonable to perform additional investigations in order to analyse this situation.

The following Figure 11 presents dependences of change of the parameters under investigation near the zone of destruction. It is clearly visible that values of SL, Sh, Rz both for the lower section and for the upper section of sample at the distances 3, 6, and 10 mm are practically equal to each other. Therefore, the stressed state within the zone of fracture is practically the same. As concerns estimation of the zone of deformation, there are good reasons to investigate digital matrices of the displayed sections (Figure 12). Due to the fact that expressions (2) and (3) are satisfied and they are valid, it is possible to determine area of the deformed section (S3) with the great degree of accuracy. In this variant, this area is equal to 119 mm^2 and it is determined in accordance with the following expression: S3 = S – S1 – S2. In this case, S, S1, and S2 are the foillowing parameters: total area of part of the image under investigation; area of the sample without any deformations; area of the image beyond the sample, respectively.

The following problems have been solved in the course of this investigation:

1. Estimation of deformation of various samples in the course of destruction on the basis of the length of the fixed section, within which fixation of such deformation occurs.

2. Determination of the law of deformation of the sample cell taking into consideration the dependence of such deformation on dimensions of this cell. These data make it possible to determine the law of deformation within the zone of destruction.

3. Investigation of the interrelationship between surface deformation of sample within the zone of destruction and the law of variation of the image intensity.

4. Determination of the zone of deformation of various materials after destruction.

4. CONCLUSIONS:

1. Mechanical tensile tests were performed. Load-displacement diagrams for all

samples under investigation were obtained. Measurements of roughness in different cross-sections before and after tests were made. Charts of changes in roughness were constructed.

2. Deformation processes in the aluminium samples in the condition of the uniaxiual static tensile were investigated in accordance with the method of correlation of digital images before and after destruction.

3. Display of the massive of the image intensity in the upper and lower parts of the fractured sample ensures visual presentation of differences or coincidences of the deformation parameters within these sections.

4. Influence of the length of the section for deformation measurements upon the value of deformation was investigated with the help of the digital method of the sample image processing.

5. The statistically significant interrelationship of the image intensity of surface of the sample under investigation with the root-mean-square deviation of the surface deformation after destruction and parameter of roughness Rz was determined.

6. Geometrical dimensions of the deformation sections near the zone of destruction are determined with the help of the method of contour analysis. In addition, this method is to be used with the help of the multivariate analysis (multi-factor analysis) of the interrelationship between image intensity, surface roughness, and possibility of determination of geometrical parameters of the deformation area/deformation volume under different conditions of operation.

5. ACKNOWLEDGMENTS:

This investigation was performed within the framework of the Russian Science Foundation grant in respect of the “Performance of investigations by scientific groups under management of young scientists” event of the Presidential Programme of the Investigation Projects (Agreement No. 19-79-10258 dated August 08, 2019).

6. REFERENCES:

1. Babaytsev, A.V., Bodryshev, V.V., Morgunova, A.A., Rabinsky, L.N. A combined method for assessing the relationship between the deformation of materials and the roughness of their surface based on digital photographs analysis of digital photographs. *Proceedings of the XXV International Symposium “Dynamic and Technological Problems of Structural Mechanics and Continuous Media” (pp. 27-28)*. Sanatorium Vyatichi, Kremenki, Russian Federation, **2019**.
2. Babaytsev, A.V., Martirosov, M.I., Rabinskiy, L.N. *Russian Metallurgy (Metally)*, **2017a**, *2017*(13), 1170-1175.
3. Babaytsev, A.V., Prokofiev, M.V., Rabonskiy, L.N. *Nanoscience and Technology: an International Journal*, **2017b**, *8*(4), 359-366.
4. Belov, P.A., Kobets, L.P., Borodulin, A.S. *Inorganic Materials: Applied Research*, **2014**, *5*(4), 403-406.
5. Berezovskii, V.V., Shavnev, A.A., Solyaev, Y.O., Lur'e, S.A., Babaytsev, A.V., Kurganova, Y.A. *News of Materials Science. Science and Technology*, **2015**, *3*, 3-10.
6. Bessonov, I.V., Polezhaev, A.V., Kuznetsova, M.N., Nelub, V.A., Buyanov, I.A., Chudnov, I.V., Borodulin, A.S. *Polymer Science – Series D*, **2013**, *6*(4), 308-311.
7. Bieda, M., Jarzębska, A., Koprowski, P., Kawałko, J., Kudłacz, K., Boczkal, S., Faryna, M., Kulczyk, M., Pachla, W., Sztwiertnia, K. *IOP Conference Series: Materials Science and Engineering*, **2018**, *375*(1), 012037.
8. Bodryshev, V.V. *Journal “Technology of materials”*, **2017**, *11*, 8-12.
9. Bodryshev, V.V., Morgunova, A.A. Digital image processing method for identifying the sizes and concentrations of phases of composite materials. *Proceedings of the 16th International Conference “Aviation and Cosmonautics – 2017” (pp. 348)*. MAI, Moscow, Russian Federation, **2017a**.
10. Bodryshev, V.V., Morgunova, A.A. Evaluation of the geometric characteristics of nanosized particles of metal oxides by digital image analysis. *Proceedings of the 16th International Conference “Aviation and Cosmonautics – 2017” (pp. 467–468).* MAI, Moscow, Russian Federation, **2017b**.
11. Borodulin, A.S. *Polymer Science – Series D*, **2013**, *6*(1), 59-62.
12. Borynyak, L.A., Nepochatov, Yu.K. *Technologies in the Electronic Industry*, **2007**, *3*, 82-88.
13. Bulychev, N.A., Kazaryan, M.A., Erokhin, A.I., Averyushkin, A.S., Rabinsky, L.N.,

Bodryshev, V.V., Garibyan, B.A. *Metal Technology*, **2018**, *9*, 39–47.

14. Dzioba, I., Lipiec, S. *IOP Conference Series: Materials Science and Engineering*, **2018**, *461*(1), 012018.
15. Faraji, G., Torabzadeh, H. *Materials Transactions*, **2019**, *60*(7), 1316-1330.
16. Filippov, A.V., Proskokov, A.V. *Bulletin of the Moscow State Technical College. N.E. Bauman, a series of "Engineering"*, **2014**, *2*, 100-113.
17. Formalev, V.F., Kolesnik, S.A. *International Journal of Heat and Mass Transfer*, **2018**, *123*, 994–998.
18. Formalev, V.F., Kolesnik, S.A. *Journal of Engineering Physics and Thermophysics*, **2017**, *90*(6), 1302-1309.
19. Görtan, M.O. *IOP Conference Series: Materials Science and Engineering*, **2017**, *194*(1), 012046.
20. Ho, H.C., Chung, K.F., Liu, X., Xiao, M., Nethercot, D.A. *Engineering Structures*, **2019**, *192*, 305-322.
21. Hosdez, J., Langlois, M., Witz, J.-F., Limodin, N., Najjar, D., Charkaluk, E., Osmond, P., Forre, A., Szmytka, F. *International Journal of Solids and Structures*, **2019**, *171*, 92-102.
22. Iwamoto, T., Kanie, S. *Procedia Engineering*, **2017**, *171*, 1272-1278.
23. Kang, J., Muhammad, W. *Journal of Testing and Evaluation*, **2017**, *45*(5), 1587-1600.
24. Khotinov, V.A., Polukhina, O.N., Vichuzhanin, D.I., Schapov, G.V., Farber, V.M. *Letters on Materials*, **2019**, *9*(3), 328-333.
25. Kobets, L.P., Malysheva, G.V., Borodulin, A.S. *Inorganic Materials: Applied Research*, **2016**, *7*(1), 15-19.
26. Kornev, Yu.V., Emelyanov, S.V., Lukyanova, A.Yu., Semenov, N.A. *Composites: Mechanics, Computations, Applications*, **2018**, *9*(4), 283-295.
27. Muniandy, K. *Materials Science and Technology (United Kingdom)*, **2019**, *35*(9), 1016-1027.
28. Pushkarev, O.I., Bochkarev, P.U., Bashkirtseva, I.V. *Procedia Engineering*, **2017**, *206*, 222-227.
29. Rabinskiy, L.N., Tushavina, O.V. *INCAS Bulletin*, **2019**, *11*(Special Issue), 203-211.
30. Rabinskiy, L.N., Tushavina, O.V., Fedotenkov, G.V. *Asia Life Sciences*, **2019**, *19*(1), 149-162.
31. Rabinsky, L.N., Tushavina, O.V. *STIN*, **2019**, *4*, 22-26.
32. Rief, T., Hausmann, J., Motsch, N. *Key Engineering Materials*, **2017**, *742*, 660-665.
33. Shtefan, E., Pashchenko, B., Blagenko, S., Yastreba, S. *Lecture Notes in Mechanical Engineering*, **2019**, 356-363. DOI: 10.1007/978-3-319-93587-4_37
34. Sodushkin, A.I., Kibitkin, V.V., Pleshanov, V.S. *Bulletin of TPU. Management, Computer Engineering and Computer Science*, **2011**, *318*(5), 48-51.
35. Vinogradov, A.A. *Bulletin of PNIPU*, **2015**, *13*, 34-39.
36. Volkov, I.V. *Computer Optics*, **2010**, *34*(1), 82-89.
37. Wang, Y., Meng, W., Xiang, D., Li, S. *Journal of Mechanical Engineering*, **2019**, *55*(1), 81-90.
38. Wu, K., Li, X., Ge, Y., Ruan, S. *International Journal of Advanced Manufacturing Technology*, **2018**, *96*(5-8), 2091-2099.
39. Yang, S.-S., Ling, X., Du, P. *Journal of Central South University*, **2018**, *25*(4), 747-753.
40. Znamenskaya, I.A., Gvozdeva, L.G., Znamensky, N.V. *Visualization methods in gas flow mechanics*, Moscow: Moscow Aviation Institute, **2001**.

$k_{discreditation} = \Delta_{measured}/\Delta_{actual.}$ (Eq.1)

$$\varepsilon = \frac{(H_{calculated} - H_{calculated\,0})}{H_{calculated\,0}}$$ (Eq. 2)

$\Delta L_{Mi} = L_{max.Mi} - L_{min.Mi/}$ (Eq.3)

$\Delta h_{ji} = h_{maxMi} - h_{minMi}$ (Eq.*4)*

$$S_{LM} = \frac{\sqrt{\sum_{1}^{k}(L_{Mk} - \overline{L_M})^2}}{k-1};$$ (Eq. 5)

$$S_{hM} = \frac{\sqrt{\sum_{1}^{n}(h_{Mn} - \overline{h_M})^2}}{n-1}.$$ (Eq. 6)

$\Delta L_1 = L_{max.} - L_{min}$ (Eq. 7)

$$a_{ij} = \begin{cases} 1, if\ L_{min} < L_i \leq L_{max} \\ 0,\ if\ L_{min} > L_i > L_{max} \end{cases}$$ (Eq. 8)

$S_i = n \times h_{cell} \times s_{cell}$ (Eq. 9)

Table 1. *Data of the relative deformation depending on the distance from the fixation jaws*

	Relative deformation ε, %		
	sample 1.1	**sample 1.2**	**sample 1.3**
complete sample	10.53	10.38	15.45
0 mm	15.58	10.38	23.61
5 mm	17.91	15.07	27.42
7 mm	19.05	18.84	29.31
9 mm	20.34	23.08	31.48
11 mm	21.82	27.87	34.00

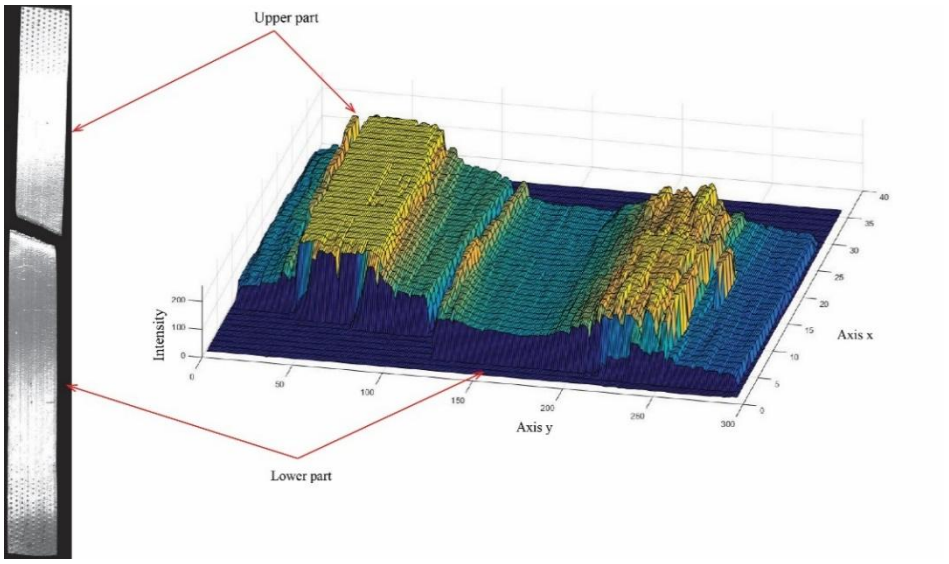

a) b)

Figure 1. *Example of surface of the metal sample, which was destroyed in the course of tensioning (a) and graphical presentation of the function L=f(x,y) of this image (b)*

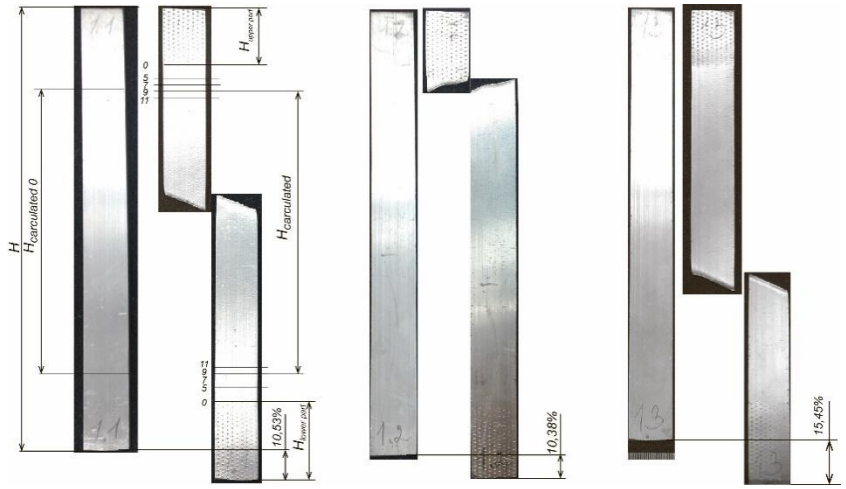

a) b) c)

Figure 2. *Superimposed images of samples before and after tensile strength tests (translations of inscriptions within the above Figure)*

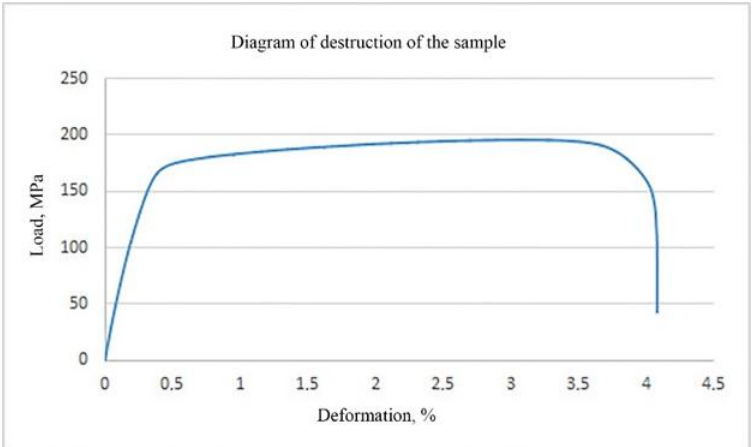

Figure 3. *Diagram of destruction of the plastic material*

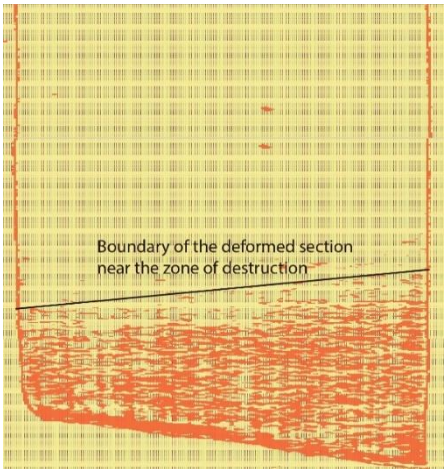

Figure 4. *Digital image of the upper part of the sample after destruction*

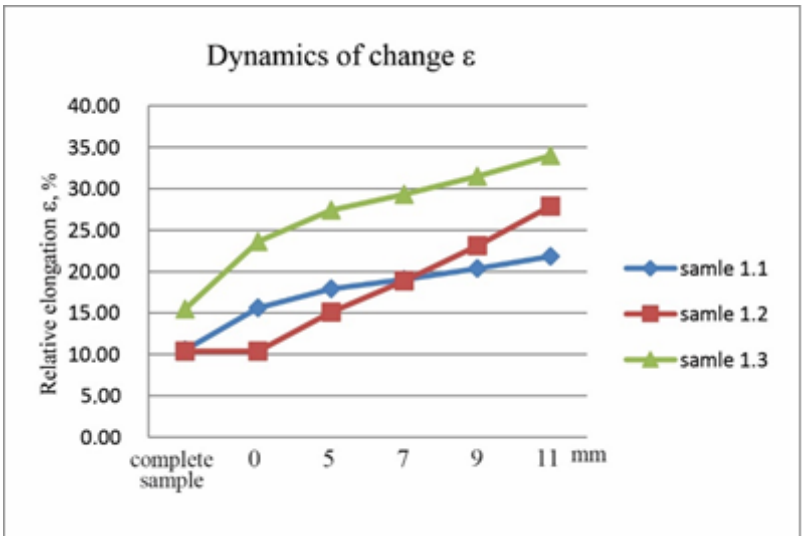

Figure 5. *Chart of change of the relative elongation of samples ε; values of the relative elongation were measured at different distances from the fixation jaws (Figure 4)*

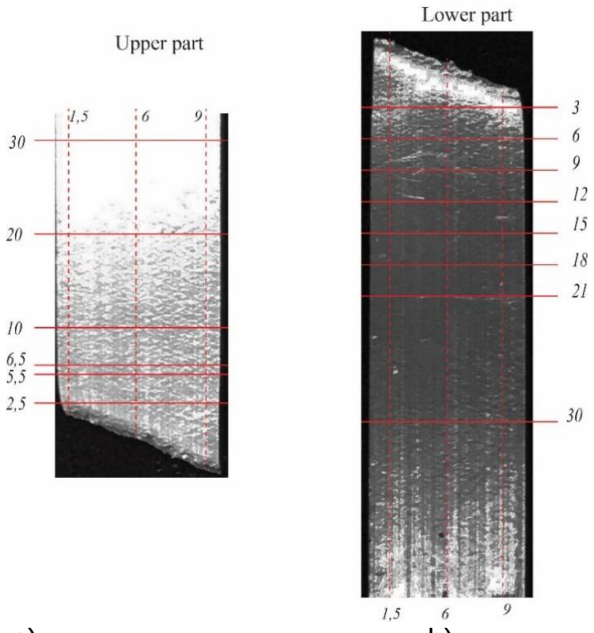

a) b)

Figure 6. *View of the fractured sample along with the preassigned cross-sections, as well as with the points of measurement of L and h values; a – the upper part; b – the lower part*

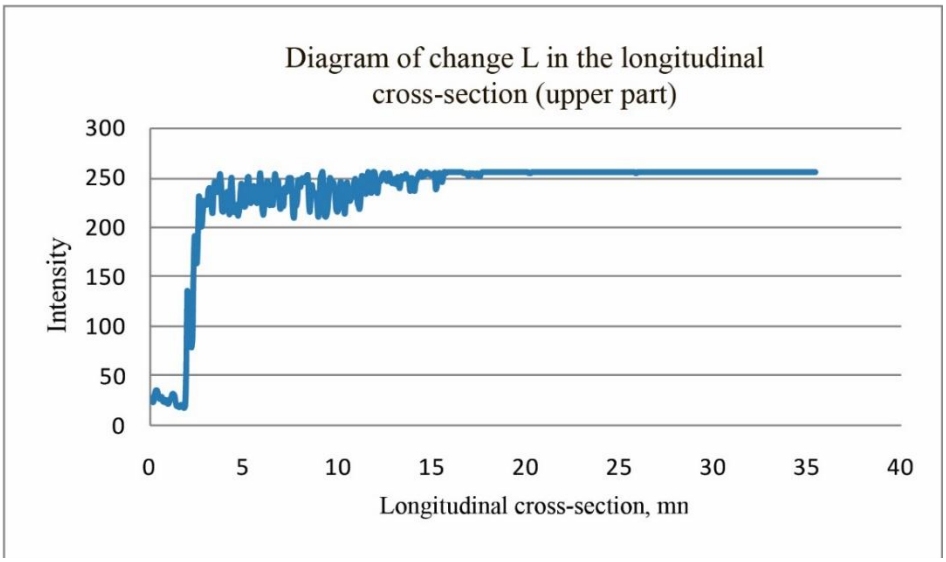

Figure 7. *Diagram of change of the image intensity in the cross-section 6*

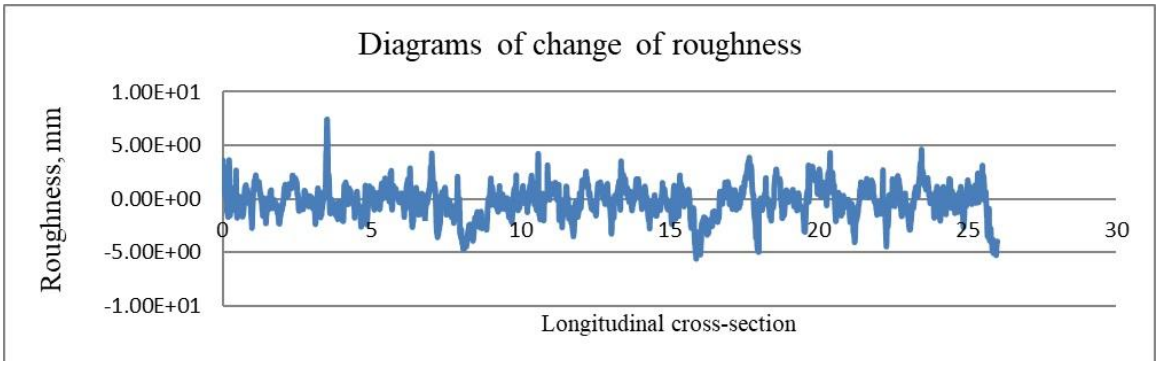

Figure 8. *Diagram of change of roughness in the cross-section 6*

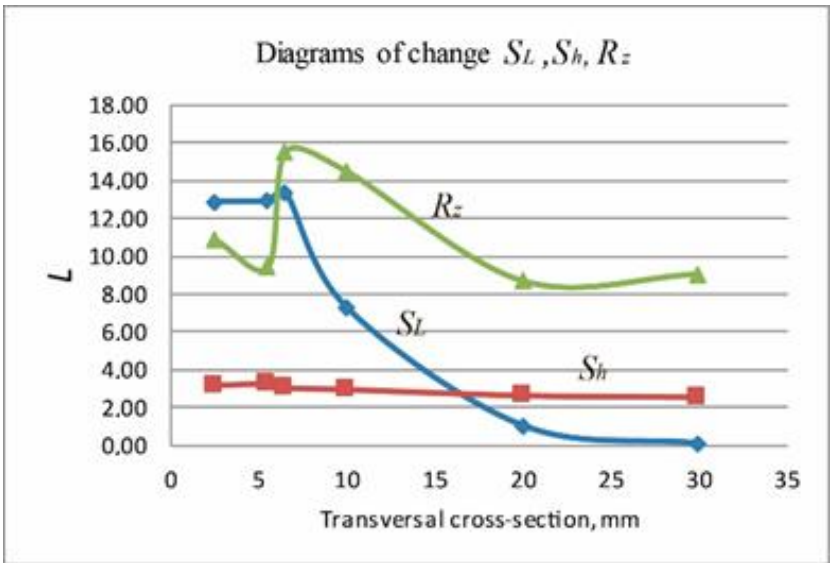

Figure 9. *Comparative diagrams of change of the data SL, Sh, and Rz in the upper part of the fractured sample*

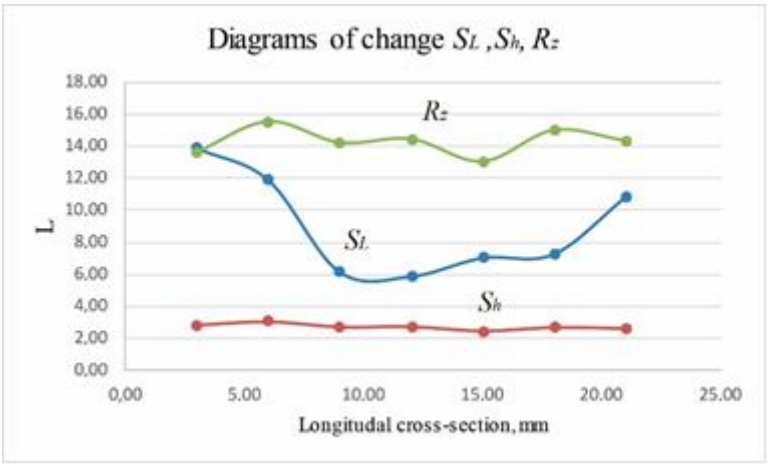

Figure 10. *Comparative diagrams of change SL, Sh, Rz in the lower part of the fractured sample*

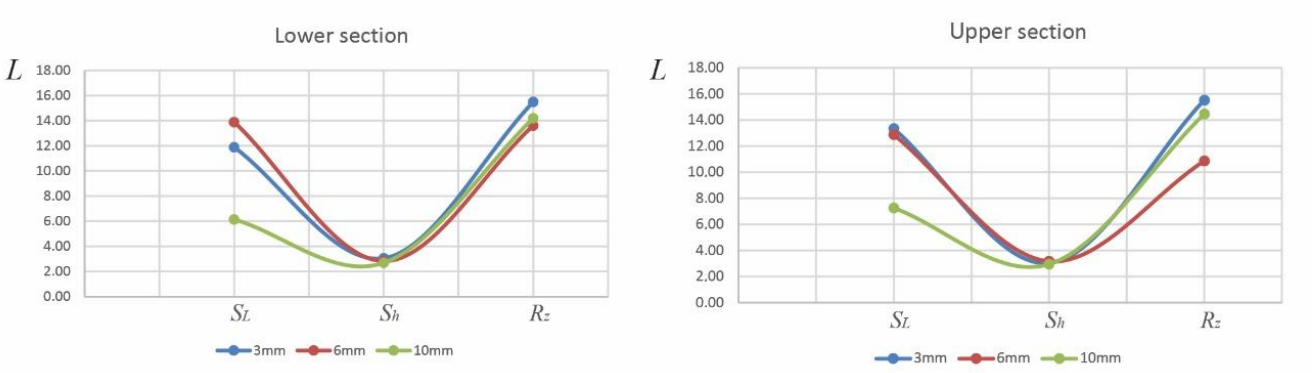

a) *b*)

Figure 11. *Diagrams of change of SL, Sh, and Rz values within the same cross-sections of the upper (a) and lower (b) sections of the destroyed sample*

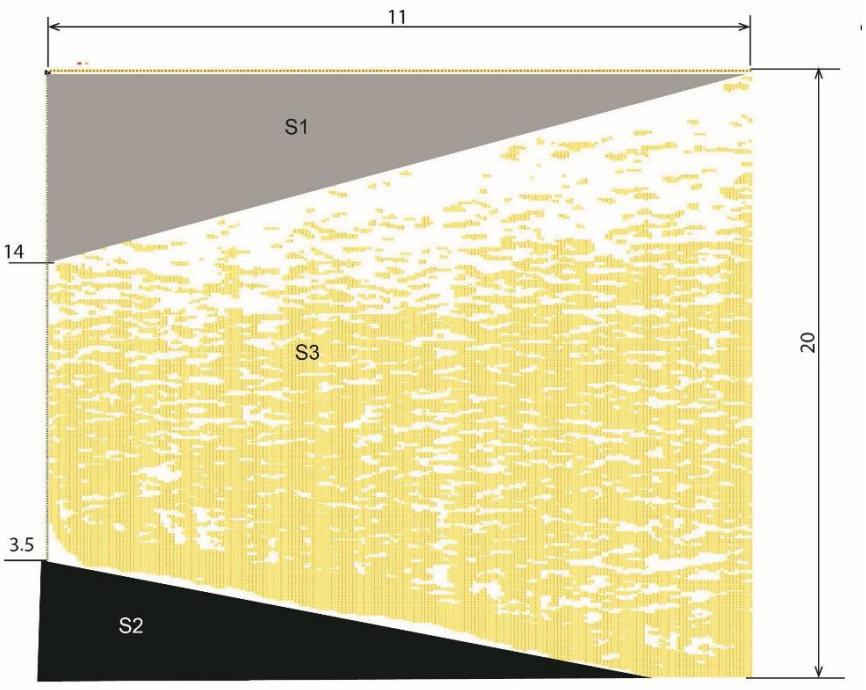

Figure 12. *Digital display of the deformed section of the fractured sample*